

1 **Load capacity of caisson anchors exposed to seabed trenching**

2
3 X. Feng¹, S. Gourvenec², D. J. White³

4
5 Manuscript submitted to Ocean Engineering

6
7
8 **¹Xiaowei FENG (corresponding author)**

9 Centre for Offshore Foundation Systems – M053

10 University of Western Australia

11 35 Stirling Highway, Crawley

12 Perth, WA 6009

13 Australia

14 Tel: +61 8 6488 2473

15 Fax: +61 8 6488 1044

16 Email: xiaowei.feng@uwa.edu.au

17
18 **²Susan GOURVENEK**

19 Faculty of Engineering and the Environment

20 University of Southampton

21 Tel: +44 (0)23 8059 9139

22 Email: susan.gourvenec@southampton.ac.uk

23
24
25 **³David J. WHITE**

26 Faculty of Engineering and the Environment

27 University of Southampton

28 Tel: +44 (0)23 8059 6859

29 Email: david.white@soton.ac.uk

30
31
32
33
34 No. of words: 6250 (without abstract and references)

35 No. of tables: 1

36 No. of figures: 17

37

38

39 **Load capacity of caisson anchors exposed to seabed trenching**

40 X. Feng, S. Gourvenec and D.J. White

41 **ABSTRACT**

42 Floating structures are often secured in position with a taut mooring system and suction
43 caissons. Large seabed trenches have been observed adjacent to some suction caisson anchors
44 with taut-line mooring systems. The trenches may jeopardise the geotechnical capacity of the
45 caissons and in turn the stationkeeping of the floating structures. Finite-element method is
46 employed to examine the geotechnical capacity of suction caissons in a trenching seabed. The
47 results show that the reduction in the geotechnical capacity becomes more significant with
48 increasing trench width due to the loss of soil support and a change in failure mechanism as the
49 caisson rotates into the trench. For a given trench width, the reduction in capacity becomes
50 more significant as the load inclination angle to the horizontal decreases. However, the shape
51 of the normalised failure envelopes for combined vertical and horizontal load is insensitive to
52 trench width. A strategy to design for inevitable trenching by moving the padeye shallower to
53 reduce the depth of trench formation is not straightforward. The gain from a shallower trench
54 may often be outweighed by the reduction in capacity from rotation of the caisson at failure for
55 loading angles typical of taut moorings.

56 **KEYWORDS**

57 caisson; trenching; failure; numerical modelling; offshore engineering;

58

59 1. INTRODUCTION

60 Suction anchors coupled with catenary or taut-line mooring systems are widely adopted to moor
61 floating facilities for offshore oil and gas developments and are a potential anchoring solution
62 for floating renewable energy facilities (Andersen et al., 2005; Tjelta, 2015; Statoil, 2015;). A
63 catenary mooring is characterised by the mooring line resting on the seabed before the anchor
64 point, while a taut line mooring reaches the anchor point at an angle, without a grounded section
65 (Figure 1). A catenary mooring forms a catenary shape in the water column from the floating
66 facility to the seabed and an inverse catenary from the seabed to the anchor chain attachment
67 point on the anchor, the padeye. Catenary moorings are typically formed from chain (or a
68 combination of chain and synthetic rope), while taut moorings are generally formed from
69 synthetic rope, which is much lighter than chain (but with short sections of chain at either end).
70 A taut line mooring will usually make an angle of 30 - 45° to the horizontal between the floating
71 facility and the padeye, with little change in the angle over the length of the line, as a result of
72 the low mass per unit length of the anchor line. Semi-taut moorings lie between the catenary
73 and taut concepts. Taut and semi-taut line moorings are attractive in deep water environments
74 to reduce the footprint of the mooring spread and improve the motion characteristics of the
75 floating system, but recent evidence suggests that the cyclic motion of the anchor line at the
76 mudline and through the seabed can contribute to the development of seabed trenches.

77 Large trenches have been observed as a result of anchor chain-soil interaction on multiple
78 offshore projects, and one of the first cases has been reported in the public domain
79 (Bhattacharjee et al., 2014). These trenches formed to the depth of the padeye and extended in
80 front of the caisson by more than twice the distance to the chain exit point at the original
81 mudline, as illustrated schematically in Figure 2. Other instances of seabed trenching have since
82 been shared in the public domain indicating the extent of the phenomenon (Sassi et al., 2017;
83 Colliat et al., 2018; O'Neill et al., 2018). The formation of the trenches is controlled by

84 mechanism similar to the trenching of steel catenary risers (Bridge and Howells, 2007). These
85 include (i) a ‘softening’ mechanism in which soil is disturbed and remoulded by the chain
86 pretension and cyclic motions; (ii) a ‘transport’ mechanism causing suspension and erosion of
87 the softened soil; and (iii) a ‘stability’ mechanism that enables the trench to remain open and
88 stable once formed, if there is an adequately high normalised shear strength (i.e. the ratio s_u/σ'_v).

89 Soil loss in the vicinity of a suction caisson has the potential to significantly reduce the
90 geotechnical capacity due to loss of support from the seabed. Optimised design of the chain
91 attachment point generally leads to translation of the caisson under the design load, but any
92 trenching effect may lead to caisson rotation, and a reduced capacity. To date, there is little
93 information available on the effect of seabed mooring line trenching on the holding capacity of
94 suction caissons for floating facilities.

95 Various analytical, numerical and experimental studies have been carried out to investigate the
96 holding capacity of suction caissons in intact seabeds, with and without a tension gap forming
97 on the active side of a caisson during rotation. The focus of much early work was the vertical
98 pullout capacity of suction caissons (Steensen-Bach, 1992; Andersen et al., 1993; Watson and
99 Randolph, 1997). A limiting equilibrium model for undrained inclined pullout capacity of
100 suction anchors was presented by Andersen and Jostad (1999). Upper bound solutions for
101 suction caisson capacity under undrained inclined load were established (Randolph and House,
102 2002; Aubeny et al., 2003) by adding new failure mechanisms to those introduced for the
103 undrained capacity of laterally loaded piles (Murff and Hamilton, 1993). The response of
104 suction caissons subjected to combined vertical and horizontal loading was investigated through
105 interaction diagrams developed with finite element analyses (Zdravkovic et al., 2001; Senders
106 and Kay, 2002; Supachawarote et al., 2004; 2005; Saviano and Pisanò, 2017). Results from an
107 industry sponsored project on a range of geotechnical design aspects of suction caissons in
108 (intact) soft clay seabeds were presented by Andersen et al. (2005). Experimental studies on

109 inclined load capacity of suction caissons, in both small scale and prototype scale models, have
110 been reported by various researchers (Andersen et al., 1993; Watson et al., 2000; Clukey et al.,
111 2003). From this previous work, procedures for analysing suction caisson capacity are well
112 established for intact seabed conditions. Disturbed seabed conditions, such as after scour or
113 sediment erosion, have also been considered in calculating the lateral resistance of the piles
114 (Achmus et al., 2010; Qi et al., 2016). A project-specific numerical study of trenching effects
115 around a suction caisson was presented by Alderlieste et al. (2016), but as yet no generalised
116 guidance is available. The viability of the finite element method to determine the load capacity
117 of suction caissons exposed to a trench was demonstrated in Sassi et al. (2018).

118 This paper examines the effect of seabed mooring line trenching on the undrained geotechnical
119 capacity of suction caisson anchors. The inclined capacities of suction caissons are obtained
120 from finite element (FE) analysis under various trenched seabed conditions. A normally-
121 consolidated fine-grained soil with linearly increasing undrained shear strength with depth is
122 considered, as relevant to deep water seabed conditions where taut-line moorings for floating
123 facilities are most prevalent. The inclined pullout capacity of a suction caisson in a trenched
124 seabed is compared to that for an intact seabed, considering variations in trench width, load
125 inclination angle and interface condition between the caisson and the seabed to represent
126 drainage that would occur following trench formation. Designing for inevitable trenching by
127 adjusting the initial padeye location is also investigated.

128 The study provides insights into governing mechanisms of failure of suction caisson anchors
129 with taut moorings in a trenched seabed through systematic study of trench geometry, loading
130 angle and drainage conditions following trench formation. The effect of out-of-plane motion of
131 the mooring line is not considered in the current work. Results are presented for a single caisson
132 aspect ratio and soil strength profile, representative of deepwater seabed conditions and

133 caissons that are most relevant to the boundary value problem under consideration. The adopted
134 conditions are based on the first published case study of anchor line trenching.

135 **2. FINITE ELEMENT MODEL**

136 All the finite element analyses presented from this study were carried out using the
137 commercially available software package ABAQUS 6.14. The general approach is consistent
138 with previous studies that have been used to define yield envelopes for caisson capacity that are
139 widely used in practice (Zdravkovic et al., 2001; Supachawarote et al., 2004; Aubeny et al.,
140 2003), and have been adopted in industry codes and guidelines (ISO, 2016). In this way, the
141 results for the no-trenched case represent a baseline consistent with current practice, and the
142 trenching is superimposed on this to identify the effect on capacity.

143 **2.1 Geometry and meshes**

144 The length-to-diameter aspect ratio of the modelled caisson is identical to that presented in the
145 published field case study (Bhattacharjee et al., 2014), and reflects the geometry of field anchors
146 at deep water sites where the seabed is susceptible to mooring line trenching (Arslan et al.,
147 2015; Alderlieste et al., 2016). The suction caisson considered has a length-to-diameter ratio of
148 $L/D = 3.11$, from a diameter of 4.5 m and length of 14.0 m. The seabed trench was taken to
149 reach the padeye depth, z_p (as observed in the field case) and the width of the trench was varied
150 according to a prescribed width-to-diameter ratio, $w/D = 0.25, 0.5, 0.75, 1.0$ and 1.25 . The
151 extent of the trench perpendicular to the caisson was assumed to be infinite. This is a reasonable
152 approach since the zone of the failure mechanism in front of the caisson does not extend as far
153 as the (finite) limit of observed seabed trenches. The problem definition is shown schematically
154 in Figure 3.

155 A typical three-dimensional finite element mesh is shown in Figure 4 for the analysis of a
156 suction caisson embedded in a seabed with a trench of width $w/D = 0.75$. Only half of the model

157 is used since symmetry exists in the plane of loading. Horizontal displacement normal to the
158 plane of symmetry (the front face in Figure 4) is prevented throughout of the analysis. The
159 meshes extended $3L$ from the edges of the caisson and $3L$ beneath the caisson tip level, with
160 horizontally constrained nodes at the sides, and fully constrained nodes at the base. The
161 boundaries were shown to be sufficiently remote so that the failure mechanism was not affected.
162 A region of very thin elements (approximately $1\%D$) was employed around the caisson
163 perimeter to ensure accurate representation of shearing along the caisson shaft (Supachawarote
164 et al., 2004) whereas the required element size, h_{uf} , adjacent to the caisson base is determined
165 as proposed by Hu and Randolph (2002)

$$\frac{h_{uf}k}{s_{u,tip}} = 0.2 \quad (1)$$

166 where k is the gradient of the soil undrained shear strength and $s_{u,tip}$ is the soil shear strength at
167 the caisson base level.

168 First order 8-node fully integrated hybrid continuum elements were used for the soil domain
169 (refer to C3D8H in the ABAQUS element library). Hybrid elements are recommended for
170 modelling the response of incompressible and near-incompressible materials (Brezzi and
171 Fortin, 2012), such as soil under undrained conditions.

172 **2.2 Material properties and interface conditions**

173 The analyses were intended to replicate the undrained response of a soft normally consolidated
174 soil with an undrained shear strength increasing proportionally with depth, z according to $s_u =$
175 kz . Normally consolidated seabeds are prevalent in deepwater locations that are most desirable
176 for taut mooring applications. The gradient of the soil undrained shear strength was adopted as
177 $k = 2$ kPa/m in this study. Although this is a higher gradient than found in the Gulf of Mexico
178 (Quiros et al 2000), it is in line with other regions where suction caissons are used (e.g. Colliat

179 et al. 2010, Erbrich & Hefer 2002). The soil was modelled as linear elastic, perfectly plastic
180 obeying a Tresca failure criterion. The elastic properties were defined by undrained Young's
181 modulus $E = 1000s_u$ and Poisson's ratio of $\nu = 0.49$ (to avoid numerical difficulties associated
182 with the constant-volume response of soil under undrained conditions). This gives a relatively
183 high rigidity index G/s_u of 336, where G is the shear modulus of the soil. The submerged unit
184 weight, γ' , of the soil was taken as 3 kN/m^3 in this study, representative of seabed deposits
185 where trenching has been observed (Ehlers et al., 2005; Colliat et al., 2010). The normalised
186 shear strength of $s_u/\sigma'_v = k/\gamma' = 0.67$ exceeds the analytical plane strain solution of 0.5 for an
187 unsupported vertical cut (Gibson and Morgenstern, 1962). The origin of the anomalously high
188 value of s_u/σ'_v might be a product of bioturbation and geochemical transformation in sediments,
189 or other features of the mineralogy and composition (Ehlers et al., 2005; Kuo and Bolton, 2013).
190 It is these conditions, where the trench can stay open as an unsupported vertical cut without
191 undrained collapse, that are relevant to mooring line trenching issues..

192 The caisson was represented as a rigid solid plug to represent an unvented cap condition, and
193 the motion of the caisson was controlled by a reference node along the midline of the caisson
194 at a depth of z_{cL} , representing the intersection of the loading vector of the mooring chain at the
195 padeye with the centreline of the caisson (Figure 3), which governs caisson response to inclined
196 loading (Randolph & House., 2002).

$$z_{cL} = z_p + \frac{D}{2} \tan\theta \quad (2)$$

197 where θ is the load inclination angle to the horizontal.

198 In the analyses, all caisson loads and displacements were applied or recovered at the reference
199 point. The submerged unit weight of the caisson foundation was assumed to be identical to that
200 of the soil. Therefore, the vertical capacity derived from the FE analyses was the net capacity
201 neglecting the submerged self-weight of the caisson.

202 The interface between the shaft of the caisson and the soil was modelled in two ways. Firstly,
203 the caisson was modelled as fully bonded to the soil, allowing unlimited tension to be mobilised,
204 representing a case of suction at the interface. Secondly, a zero tension interface was modelled,
205 to allow the possibility of loss of suction forming at the interface. Gap formation is a design
206 concern, since the presence of a seabed trench may accelerate the dissipation of the negative
207 excess pore pressure around the caisson, preventing suction being maintained on the active face
208 and therefore eliminating any interface tension.

209 The normal behaviour of the zero-tension interface was modelled by ‘hard’ contact with no
210 tensile stress transmitted, and the tangential behaviour was represented by the Coulomb
211 frictional contact with coefficient of friction of 1.0. The underside of the caisson was fully
212 bonded to the soil with no detachment allowed, representing the ‘soil-soil’ interface between
213 the soil plug and the underlying soil.

214 **2.3 Analysis procedure**

215 The caisson was pre-embedded without considering the effect of installation. The geostatic
216 stresses of the soil were initially established for the intact seabed condition, with a set of
217 elements at the location where the trench would subsequently be formed. The development of
218 the seabed trench was simulated by deactivating the predefined elements in the trenched zone
219 with the model change function in ABAQUS. For the particular case of the instant of trench
220 development, the out-of-plane displacement constraint over the trenched zone at the plane of
221 symmetry in the model for intact seabed ($w/D = 0$) was released to simulate an infinitesimally
222 narrow trench. Following trench development, an external load was applied to the suction
223 caisson at the reference node by either imposing a displacement or a directly applied force to
224 bring the caisson to failure and the load capacity was determined.

225 **2.4 Load path**

226 For cases when the caisson body was free to rotate, a concentrated force or a displacement was
227 specified at the reference point along the direction of the prescribed load inclination. The
228 maximum capacity of the caissons was determined by prescribing translation without rotation,
229 in practice achieved by moment equilibrium from the optimal combination of padeye depth and
230 loading angle for the particular caisson geometry and undrained shear strength profile.

231 **3. RESULTS**

232 The finite element model was validated by considering the pure vertical pullout capacity and
233 translational capacity of the suction caisson embedded in an intact seabed, i.e. $w/D = 0$.
234 Subsequently, the load capacity of the suction caisson in trenched seabeds is presented for the
235 padeye located at the designated depth of 9 m (Bhattacharjee et al., 2014). Finally, the influence
236 of padeye offset is discussed to examine the effect of the trench depth on capacity.

237 **3.1 Caisson load response verification-Intact seabed**

238 *Vertical pullout capacity*

239 The undrained vertical pullout capacity of a caisson in an intact seabed consists of the shearing
240 resistance along the caisson shaft and the reverse end bearing resistance at tip level. For the
241 conditions modelled, shaft resistance can be deduced from the product of the shaft surface area
242 and the average shear strength over the embedded depth modified by a soil-structure interface
243 factor. The base resistance was estimated by subtracting the theoretical shaft resistance from
244 the total load obtained from the vertical pullout analyses. The end bearing factor N_c can be
245 calculated according to

$$N_c = \left(V_{ui} - \pi D \int_0^L \alpha s_u dz \right) / A s_{u,tip} \quad (3)$$

246 Where

247 V_{ui} = ultimate pullout force at failure (taken as the force at a displacement of $0.1D$ at a plastic
248 plateau)

249 A = cross sectional, bearing, area of the caisson

250 α = interface friction ratio, taken as 1 for full caisson-soil adhesion.

251 The computed value of N_c is approximately 10.9, compared with 10.5 for length-to-diameter
252 L/D greater than 3 based on two-dimensional axisymmetric finite-element analyses reported by
253 Aubeny et al. (2003).

254 *Horizontal translation capacity*

255 The translational capacity of a suction caisson derives from the shearing across the base at tip
256 level, potentially a deep flow-around mechanism above toe level, and a wedge-type failure of
257 the soil at shallow depths (Figure 5). The soil resistance mobilised by the soil wedges is
258 governed by the gapping conditions, which are relevant to the caisson-soil interface properties.
259 Under the zero-tension interface (ZTI) condition, a gap may form on the active side of the
260 caisson. The soil resistance for such a one-sided wedge mechanism is only due to the shear
261 strength and weight of the passive wedge in front of the caisson. For the case of an unlimited
262 tension interface (UTI) where a gap cannot form, the soil resistance due to the shear strength of
263 the passive and active wedges is equal for a two-sided mechanism, but the resistance associated
264 with the weight of the wedges cancels out.

265 The lateral capacity of the caisson, excluding base shearing, may be assessed using the profiles
266 of lateral resistance factor, N_p , derived from the plasticity solution for a one-sided mechanism

267 proposed by Murff and Hamilton (1993). An approximate fit of Equation (4) based on the
268 analytical solution was suggested for the variations of N_p with depth (Figure 5).

$$N_p(z) = N_1 - N_2 e^{-\xi z/D} \quad (4)$$

269 where N_1 is the limiting bearing factor at depth, varying with interface friction from 9.14 for a
270 smooth caisson, to 11.94 for a fully rough caisson (Martin and Randolph, 2006). N_2 is selected
271 such that $(N_1 - N_2)$ is the capacity factor at the intercept at the soil surface, being 2.82 and 2 for
272 a rough and smooth caisson, respectively (Aubeny et al., 2003). The decay factor, ξ ,
273 characterises the effect of soil strength profile, expressed as

$$\xi = 0.25 + 0.05 \text{Min}(6, s_{um}/kD) \quad (5)$$

274 where s_{um} is the soil undrained strength at mudline and k is the strength gradient.

275 Assuming a two-sided mechanism with no gap for full caisson-soil adhesion, the value of N_p
276 needs to be doubled, subject to the restriction that N_p does not exceed the limiting value at
277 depth, N_1 (Aubeny et al., 2003).

278 The normalised horizontal capacity factor for a translating caisson N_h is defined as

$$N_h = (H_{ui} - A s_{u,tip}) / L D s_{u,avg} \quad (6)$$

279 Where H_{ui} is the ultimate horizontal capacity for a translational caisson and $s_{u,avg}$ is the average
280 soil shear strength over the depth of caisson embedment. The value of N_h derived from the FE
281 analysis is 10.9 for UTI, 4.4% lower than the upper bound solution of 11.4, whereas the FE
282 result of N_h is 7.5 for ZTI condition, 8.7% higher than the analytical solution of 6.9 using the
283 N_p profile provided in Equation (4).

284 3.2 Effect of trench on vertical pullout and translational capacity

285 The reduction ratio of pure pullout, V_u , and translational load capacity, H_u , in the trenched
 286 seabed compared to the intact seabed is shown in Figure 6 for UTI, (i.e. full suction maintained)
 287 and ZTI (i.e. no suction permitted behind the caisson due to possible rapid drainage to the
 288 trench) cases, as a function of trench width. The trench is assumed to develop to the level of the
 289 padeye, located at $0.64L$, consistent with the optimal position for a taut-line system in a
 290 normally consolidated intact seabed. The changes in pure vertical and horizontal capacities are
 291 not intended to represent or inform on potential uniaxial failure mechanisms in the field but to
 292 provide insight into effects of trenching on these idealised cases as a basis for considering
 293 inclined loading.

294 Figure 6 shows that both vertical and translational capacities reduce with increasing trench
 295 width and the loss of suction behind the caisson, more significantly for translational capacity.
 296 The undrained vertical pullout capacity of caissons in a trenched seabed consists of the shearing
 297 resistance along the caisson shaft and the reverse end bearing resistance at tip level, identical
 298 to in an intact seabed. The shaft resistance during pullout decreased in the trenched seabed due
 299 to the reduced contact area between the caisson and the seabed. The end resistance factor
 300 considering the trenched soil can be predicted by Equation 7, accounting for the shaft area
 301 affected by the trench, as

$$N_c = \left(V_u - \pi D \int_0^L \alpha s_u dz + D \sin^{-1} \int_0^{z_p} \alpha s_u dz \right) / A_{S_{u,tip}} \quad (7)$$

302 The end resistance factor N_c of the caissons in a trenched seabed, presented in Figure 7, is
 303 practically identical with that in the intact seabed irrespective of the interface condition,
 304 indicating that the effect of the trench on end bearing resistance is minimal despite the reduced
 305 overburden. Therefore, the reduction of the pullout capacity is induced by loss of caisson
 306 surface area in contact with soil. For the case where suction is lost on the caisson-soil interface,

307 the reduction in vertical capacity becomes more significant as the trench width increases, since
308 the caissons rotates more significantly into the trench at the stage of trench development,
309 leading to more loss of contact and therefore shaft resistance in the following uplift.

310 The reduction in translational capacity for a trenched seabed shown in Figure 6 and the
311 calculated normalised horizontal capacity factor N_h , from Equation 6, is plotted in Figure 7.
312 The reduction in the translational capacity is caused by the loss of soil in the trenched zone and
313 the change in the soil flow mechanism around the caisson. The soil flow mechanisms for the
314 UTI and ZTI are illustrated in Figure 8 and Figure 9, respectively. A step fall in H_u for the UTI
315 ($\sim 10\%$) and ZTI ($\sim 15\%$) is evident for $w/D \rightarrow 0$, i.e. for an infinitesimally narrow trench even
316 though the same volume of soil is present around the caisson. This immediate reduction in
317 capacity is because any trench removes the potential for tensile resistance across the front of
318 the caisson, with this wound weakening the soil support. Figure 8a and b show the abrupt
319 change in the soil flow mechanism on the front side of the caisson with UTI for an intact seabed
320 and $w/D \rightarrow 0$. The scenario of $w/D \rightarrow 0$ is not intended to represent a physical reality, but is
321 examined to demonstrate the significant effect of the change of the soil failure mechanism, as
322 shown in Fig.8b, and explain the step change (rather than smooth transition) in the load capacity
323 of the caisson when the seabed transitions from intact into trenched conditions.

324 In the absence of the active soil wedge, Figure 9a and b demonstrate a similar immediate
325 transition in mechanism at the passive side for caissons with ZTI. As the trench widens to w/D
326 $= 1$, H_u reduces respectively to $\sim 70\%$ and $\sim 53\%$ of the untrenched value for the UTI and the
327 ZTI, as the volume of soil in the failure mechanism progressively reduces.

328 For the zero tension interface, the gap on the active side extends to the caisson tip and the soil
329 wedge does not mobilize owing to the soil detachment. The difference in N_h between ZTI and
330 UTI conditions is essentially independent of trench width (see Table 1), since it is governed by

331 the contribution of the soil resistance mobilised on the active side of the caisson, away from the
332 trench. The discrepancy accounts for 31% (< 50%) of the untrenched value for UTI due to the
333 contribution of the soil weight on the active side.

334 The case of an infinitesimally narrow trench is only of theoretical interest but shows that the
335 trench affects H_u via two distinct effects – (i) elimination of tensile resistance ahead of the
336 caisson, and (ii) a reduction in the overall volume of deforming soil.

337 **3.3 Inclined load capacity of caissons - Effect of trench width**

338 The results above have shown that the presence of a seabed trench reduces the pullout and
339 translational capacity of suction caissons due to the absence of resistance from the soil in the
340 trenched zone and loss of suction on the caisson/soil interface. In this section, the effect of the
341 trench on the inclined load resistance, F_u , is presented, demonstrating the additional reduction
342 in capacity due to the possible rotation of the suction caisson in a trenched seabed, as opposed
343 to a pure translational mechanism that the caisson would have been designed for considering
344 an intact seabed.

345 Results are presented in terms of a reduction factor, defined as the ratio of the geotechnical
346 capacity of the caisson in the trenched seabed F_u to that in the intact seabed F_{ui} . All curves
347 except those for $\theta = 90^\circ$ in Figure 10 converge to $F_u/F_{ui} < 1$ for trench width $w/D \rightarrow 0$. This is
348 because an infinitesimally thin trench is responsible for eliminating tension across the front of
349 the caisson – as shown in Figure 6 for pure horizontal loading ($\theta = 0^\circ$).

350 Figure 10 illustrates the components of reduction in capacity separated by (i) loss of suction
351 behind and soil support in front of the caisson, and (ii) rotation of the caisson. Effect (i) is
352 derived by constraining rotation while modelling the trench depth at the level of the padeye
353 corresponding to the optimal loading point for each chain angle for an intact seabed (Figure
354 10a). The load-capacities shown in Figure 10b represent caissons embedded in the trenched

355 seabed with rotation permitted and the load applied at the depth where no rotation would occur
356 for an intact seabed. The reduction in capacity becomes increasingly significant as the trench
357 width increases and for load inclination angles of $\theta < 60^\circ$, and is more significant for the case
358 of loss of suction on the caisson/soil interface. The greater reduction in capacity due to rotation
359 arises from effect (ii), because the depth of intersection of the loading vector at the caisson
360 centreline that causes pure translation, z_0 , becomes deeper with increasing trench width, as
361 shown in Figure 11. Therefore, the optimal padeye position for the intact seabed condition is
362 not optimal for the trenched seabed. Instead, it is too shallow and induces forward rotation of
363 the caisson. For the case of zero-tension interface, the soil resistance due to the active wedge is
364 absent, and the moment attributed to the passive soil wedge must equilibrate that associated
365 with the tip sliding to achieve the translating mechanism. Therefore, the optimal load
366 intersection with the centreline becomes deeper than that for the case of UTI. Additional checks
367 confirm that the value of z_0 presented in Figure 11 are insensitive to the adopted gradient of the
368 undrained shear strength, k , for given seabed and interface conditions.

369 The reduction in the capacity caused by free rotation compared with the translating caisson is
370 minimal for loading with a significant vertical component, $\theta > 60^\circ$. An example of the
371 dependence of capacity on loading angle θ is shown in Figure 12 as a function of the depth to
372 the load intersection point at the centreline of a caisson for the case of UTI, and embedded in
373 a trenched seabed with $w/D = 0.25$. Figure 12 indicates that for the load inclination angle $\theta < \sim$
374 60° to the horizontal, the capacity is highly sensitive to the intersection of the loading vector
375 with the centreline as the transition in mechanism from translational to rotational is abrupt. For
376 load inclination angles greater than 60° to the horizontal, where the caisson failure is governed
377 by the vertical pullout, the capacity is only marginally reduced over a relatively wide range of
378 load attachment depths.

379 The capacity of the suction caissons for any given load inclination angle can be determined
 380 from a V-H interaction diagram. The V-H capacity for caissons in a trenched seabed is
 381 presented in Figure 13a and b with respect to that in an intact seabed for UTI and ZTI,
 382 respectively. The dotted lines show the capacity for caissons permitted to rotate (as would occur
 383 in the field in the presence of trenching), with the load applied at the optimal attachment point
 384 for the intact seabed. The solid lines are the failure envelopes for the translating caissons, shown
 385 to highlight the separate effects of (i) loss of soil support in front of the caisson and (ii) the
 386 change of failure mechanism from translation to rotation. The capacity under inclined loading
 387 reduces with increasing trench width, w/D and for loading angles dominated by a horizontal
 388 component. For typical taut-line mooring angles, $30^\circ \leq \theta \leq 45^\circ$ to the horizontal, a trench as
 389 wide as the caisson diameter causes a reduction in capacity to 60% - 75% of the optimal capacity
 390 in an intact seabed for the conditions modelled. If suction is lost on the active side of the caisson,
 391 the capacity for $w/D = 1.0$ would reduce more significantly to 36% - 42% of the optimal value
 392 for untrenched seabed.

393 The normalised V-H failure envelopes are plotted in Figure 14a for unlimited tension interface
 394 conditions (UTI), revealing that the shape of the failure envelope is insensitive of the trench
 395 width and the mode of caisson motion. A general ellipse defined for intact seabed and aspect
 396 ratio of $1.5 < L/D < 5.0$ can be used to describe the failure envelopes (Supachawarote et al.,
 397 2004):

$$\left(\frac{H}{H_u}\right)^{0.5+L/D} + \left(\frac{V}{V_u}\right)^{4.5-L/3D} = 1 \quad (8)$$

398 For the case of ZTI, the shape of the failure envelope is independent of the trench width, but is
 399 (slightly) affected by whether the caisson is constrained to translate or free to rotate for load
 400 inclination angle $\theta < 45^\circ$.

401 3.4 Padeye offset for optimal capacity in a trenched seabed

402 The location of the padeye determines the maximum trench depth as well as the capacity and
 403 mode of failure of the caisson. It is therefore worth consideration if the location of the padeye
 404 can be optimized assuming trench formation down to padeye depth is inevitable. There is a
 405 trade-off between locating the padeye at a shallower than optimal depth (for the intact seabed
 406 case), thereby accepting a rotational failure mode, in order to reduce the depth to which the
 407 trench develops. In this section, the effect of trench depth or adjustment of the location of the
 408 padeye is discussed.

409 Figure 11 compares the locations of the optimal load intersection point at the centreline of the
 410 caisson for various padeye positions which change from the mid-height of the caisson
 411 embedment, i.e. $z_p/L = 0.5$, to the depth to optimal load intersection with the centreline for an
 412 intact seabed, i.e. $z_p/L = 0.7$ for UTI and 0.73 for ZTI. The depth to the optimal load intersection
 413 with the caisson centreline increases as the trench width increases regardless of the interface
 414 properties. For given trench width, the reduction of the depth to the optimal load intersection
 415 with the centreline is minimal for caissons with UTI. The reason is that the soil reaction force
 416 P_a against the active side of the caisson and the sliding resistance P_{tip} at the caisson tip are
 417 virtually unaffected by the presence of the seabed trench, whereas the passive soil reaction force
 418 P_p increases for a shallower trench depth, but the corresponding moment arm decreases so that
 419 the position of the optimal load intersection point at caisson centreline (point O) shifts slightly
 420 to achieve the moment equilibrium for a translating mechanism (Figure 15).

$$P_p L_p + P_{tip} L_t = P_a L_a \quad (9)$$

421 where P_p , P_{tip} and P_a respectively are the forces acting on the passive side, tip and active side of
 422 the caisson, with L_p , L_t and L_a being the corresponding moment arm with respect to O. Even
 423 though the reduction of the depth to the optimal load intersection with the centreline is more

424 significant for caissons with zero-tension interface than that for UTI (Figure 11), it is still
425 considerably smaller compared with the padeye offset, leading to forward rotation of the caisson
426 for the loading direction at the padeye. Therefore, the gain in the geotechnical capacity of the
427 caisson from a shallower trench might be outweighed by the reduction owing to caisson
428 rotation.

429 The load capacity of caissons in seabeds with various depths of mooring line-induced trenches
430 is presented in Figure 16, where the trench depth varies according to the prescribed load
431 intersection point at the caisson centreline, z_{cL} and load inclination angle, θ . Moving the padeye
432 to a shallower depth does not necessarily lead to a higher geotechnical capacity for load
433 inclination angles less than or equal to 45° to the horizontal, most relevant to taut or semi-taut
434 mooring systems. With a full tension interface, i.e. suction maintained on the passive side of
435 the caisson, the geotechnical capacity for a caisson with loading angle $\theta = 30^\circ$ and trench width
436 $w/D = 1.0$ reduced by 7% as the depth of the padeye decreased from $0.68L$ to $0.61L$. If suction
437 is lost on the active side of the caisson, the load capacity for $\theta = 45^\circ$ can reduce 10% with the
438 trench depth decreased from $0.68L$ to $0.54L$. This is because the geotechnical capacity of the
439 caisson is very sensitive to the position of the load intersection point at the centreline for small
440 load inclination angles. For load inclination angles exceeding 75° to the horizontal, vertical
441 pullout dominates the failure and the reduction in the geotechnical capacity results from the
442 loss of contact rather than the change in the failure mechanism of the caisson. The geotechnical
443 capacity is lower for any trench width as the trench depth increases, as would be expected. The
444 results presented in Figure 16c show that the capacity varies in approximate proportion to the
445 trench width.

446 4. APPLICATION OF RESULTS TO CASE STUDY

447 The results of this study indicate that when the trench geometry observed in front of the
448 Serpentina suction caissons (Bhattacharjee et al. 2014) is considered in the present analysis, the
449 holding capacity of any individual caisson is reduced by up to 65% for a trench as wide as the
450 caisson diameter ($w/D = 1$), compared to the optimal capacity assuming an intact seabed and
451 location of the padeye, $z_p/L = 0.64$, to mobilize a translational failure mechanism (Figure 17).

452 Moving the padeye to a shallower position to reduce the trench depth would not have increased
453 the holding capacity above the trenched capacity at the original padeye depth. This is because
454 the gain from the reduced trench depth is exceeded by loss in capacity from transition to a
455 rotational mechanism for these conditions.

456 The design capacity could be achieved by various combinations of increased caisson diameter
457 and/or length and padeye location. One example is to maintain the original loading angle,
458 caisson aspect ratio, and aim to achieve the design capacity indicated in Figure 17, which
459 corresponds to pure translation in an intact seabed with the actual anchor dimensions. This
460 capacity would require the caissons to be 7.14 m in diameter and 22.2 m in length with a padeye
461 at mudline. This represents a significant increase in size compared to the original dimensions
462 of $D = 4.5$ m, $L = 14.0$ m with depth to padeye $z_p = 9$ m, to overcome the challenge of seabed
463 trenching.

464 5. CONCLUSIONS

465 This paper has examined the load capacity of suction caisson anchors exposed to anchor line
466 seabed trenching through finite-element analyses. The effect of a range of in-line load paths,
467 interface conditions and trench configurations have been considered with reference to selected
468 caisson geometry and soil profile, representative of field caissons and deep water seabed
469 conditions, most relevant to the taut line mooring concept. This study has illustrated the

470 significant effect of anchor line seabed trenching on caisson capacity for taut-line mooring
471 systems and the variables that are significant to reduction in caisson capacity.

472 The analyses have revealed that:

473 • The reduction in vertical pull-out capacity is attributed to the loss of shaft resistance due
474 to the trenched soil. For cases where suction is still mobilised at the caisson/soil interface away
475 from the trenched area the undrained uplift capacity in the trenched seabed was generally 10%
476 lower than compared with an intact seabed. In contrast, in cases where suction was lost at the
477 caisson/soil interface due to the reduced drainage path length following trench formation, the
478 vertical capacity for caissons reduces further as the trench width increases owing to greater loss
479 of contact at the caisson/soil interface. The soil end resistance at caisson tip level was not
480 significantly affected by the presence of the trench.

481 • Maximum horizontal capacity, i.e. mobilised under pure translation, was reduced by ~
482 40% and ~ 70% as the trench width w/D reached unity for cases where suction at the caisson/soil
483 interface was maintained or lost, respectively. The significant loss of capacity is attributed to a
484 combination of the loss of soil support in the trenched zone and transition to a non-optimal
485 rotational failure mechanism as the initial optimal depth of the padeye for an intact seabed
486 becomes non-optimal in the presence of the trench, leading to rotation of the caisson.

487 • The reduction in inclined capacity of the suction caisson increased as the load angle to
488 the horizontal decreased. The reduction in capacity was most significant for mooring line angles
489 less than 60° to the horizontal – noting that most taut line mooring systems have loading angles
490 between 30° and 45°. For loading angles > 75°, the failure mechanism is dominated by uplift.

491 • The shape of the normalised V-H failure envelopes was insensitive to the normalised
492 trench width.

493 • The optimal depth to the load intersection point at the caisson centreline increased as
494 the trench width increased and suction was lost on the active side. Improvement in geotechnical

495 capacity by changing the padeye position to reduce trench depth was negligible because gains
496 in capacity from a reduced trench depth were offset by reduction in capacity due to transition
497 to a rotational mechanism.

498 Thus, in seabeds with a risk of anchor line trenching, anchor size must be increased in order to
499 achieve the same design capacity. A range of combinations of caisson length and diameters
500 along with loading angles could offer the target capacity, and drivers to narrow the selection of
501 variables are likely to be project specific. In areas where trenching has been observed, a
502 catenary mooring spread could be adopted and the larger footprint accommodated to minimize
503 risk of trenching.

504 **6. ACKNOWLEDGEMENTS**

505 This work was supported by the ARC Industrial Transformation Research Hub for Offshore
506 Floating Facilities which is funded by the Australian Research Council, Woodside Energy,
507 Shell, Bureau Veritas and Lloyds Register (Grant No. IH140100012). The work forms part of
508 the activities of the Centre for Offshore Foundation Systems (COFS), established in 1997 under
509 the Australian Research Council's Special Research Centres Program, and supported as a node
510 of the Australian Research Council's Centre of Excellence for Geotechnical Science and
511 Engineering (CE110001009).

512 **REFERENCES**

513 Achmus, M., Kuo, Y.-S., Abdel-Rahman, K., 2010. Numerical investigation of scour effect on
514 lateral resistance of windfarm monopiles. In: Proc of The Twentieth International Offshore and
515 Polar Engineering Conference. ISOPE, Beijing, China, pp. 619-623.
516 Alderlieste, E., Romp, R., Kay, S., Lofterød, A., 2016. Assessment of Seafloor Trench for
517 Suction Pile Moorings: a Field Case. In: Proc of Offshore Technology Conference. OTC,
518 Houston, Texas, OTC-27035-MS.
519 Andersen, K., Murff, J., Randolph, M., Clukey, E., Erbrich, C., Jostad, H., Hansen, B., Aubeny,
520 C., Sharma, P., Supachawarote, C., 2005. Suction anchors for deepwater applications. In: Proc
521 of the 1st International Symposium on Frontiers in Offshore Geotechnics (ISFOG 2005), Perth,
522 Australia, pp. 3-30.

- 523 Andersen, K.H., Dyvik, R., Schröder, K., Hansteen, O.E., Bysveen, S., 1993. Field tests of
524 anchors in clay II: predictions and interpretation. *Journal of Geotechnical Engineering* 119 (10),
525 1532-1549.
- 526 Andersen, K.H., Jostad, H.P., 1999. Foundation design of skirted foundations and anchors in
527 clay. In: *Proc of Offshore Technology Conference*. OTC, Houston, Texas, OTC-10824-MS.
- 528 Arslan, H., Peterman, B.R., Wong, P.C., Bhattacharjee, S., 2015. Remaining Capacity of the
529 Suction Pile due to Seabed Trenching. In: *Proc of the 20th International Offshore and Polar
530 Engineering Conference*. ISOPE, Hawaii, USA, pp. 924-931.
- 531 Aubeny, C., Han, S., Murff, J., 2003. Inclined load capacity of suction caissons. *International
532 Journal for Numerical and Analytical Methods in Geomechanics* 27 (14), 1235-1254.
- 533 Bhattacharjee, S., Majhi, S.M., Smith, D., Garrity, R., 2014. Serpentina FPSO Mooring
534 Integrity Issues and System Replacement: Unique Fast Track Approach. In: *Proc of Offshore
535 Technology Conference*. OTC, Houston, Texas, OTC-25449-MS.
- 536 Brezzi, F., Fortin, M., 2012. *Mixed and hybrid finite element methods*. Springer-Verlag New
537 York, New York.
- 538 Bridge, C.D., Howells, H.A., 2007. Observations and modeling of steel catenary riser trenches.
539 In: *Proc of the 7th International Offshore and Polar Engineering Conference*. ISOPE, Lisbon,
540 Portugal, pp. 803-813.
- 541 Clukey, E.C., Aubeny, C.P., Murff, J.D., 2003. Comparison of analytical and centrifuge model
542 tests for suction caissons subjected to combined loads. In: *Proc of the 22nd International
543 Conference on Offshore Mechanics and Arctic Engineering*. American Society of Mechanical
544 Engineers, pp. 889-894.
- 545 Colliat, J.-L., Safinus, S., Boylan, N., Schroeder, K., 2018. Formation and Development of
546 Seabed Trenching from Subsea Inspection Data of Deepwater Gulf of Guinea Moorings. In:
547 *Proc of Offshore Technology Conference*. OTC, Houston, Texas, OTC-29034-MS.
- 548 Colliat, J., Dendani, H., Puech, A., Nauroy, J., 2010. Gulf of Guinea deepwater sediments:
549 Geotechnical properties, design issues and installation experiences. In: *Proc of the 2nd
550 International Symposium on Frontiers in Offshore Geotechnics (ISFOG 2010)*, Perth, Australia,
551 pp. 59-86.
- 552 Ehlers, C., Chen, J., Roberts, H., Lee, Y., 2005. The origin of near-seafloor crust zones in
553 deepwater. In: *Proc of the 1st Int. Symp. on Front. in Offshore Geotech. (ISFOG 2005)*. Taylor
554 and Francis, Perth, Australia, pp. 927-934.
- 555 Gibson, R.E., Morgenstern, N., 1962. A Note on the Stability of Cuttings in Normally
556 Consolidated Clays. *Géotechnique* 12 (3), 212-216.
- 557 Hu, Y., Randolph, M.F., 2002. Bearing capacity of caisson foundations on normally
558 consolidated clay. *Soils and Foundations* 42 (5), 71-77.
- 559 ISO, 2016. *Petroleum and natural gas industries specific requirements for Offshore Structures
560 - Part 4: Geotechnical and foundation design considerations - 2nd Edition*. International
561 Organization for Standardization, Geneva.
- 562 Kuo, M., Bolton, M., 2013. The nature and origin of deep ocean clay crust from the Gulf of
563 Guinea. *Géotechnique* 63 (6), 500-509.
- 564 Martin, C.M., Randolph, M.F., 2006. Upper-bound analysis of lateral pile capacity in cohesive
565 soil. *Géotechnique* 56 (2), 141-145.
- 566 Murff, J.D., Hamilton, J.M., 1993. P-ultimate for undrained analysis of laterally loaded piles.
567 *Journal of Geotechnical Engineering* 119 (1), 91-107.
- 568 O'Neill, M., Erbrich, C., McNamara, A., 2018. Prediction of Seabed Trench Formation Induced
569 by Anchor Chain Motions. In: *Proc of Offshore Technology Conference*. OTC, Houston, Texas,
570 OTC-29068-MS.
- 571 Qi, W.G., Gao, F.P., Randolph, M.F., Lehane, B.M., 2016. Scour effects on p-y curves for
572 shallowly embedded piles in sand. *Géotechnique* 66 (8), 648-660.

- 573 Randolph, M., House, A., 2002. Analysis of suction caisson capacity in clay. In: Proc of
574 Offshore Technology Conference. OTC, Houston, Texas, OTC-14236-MS.
- 575 Sassi, K., Kuo, M., Versteede, H., Cathie, D., Zehzouh, S., 2017. Insights into the Mechanisms
576 of Anchor Chain Trench Formation. In: Proc of the 8th Offshore Site Investigations and
577 Geotechnics Conference, Society for Underwater Technology (OSIG 2017). Society of
578 Underwater Technology, London, UK, pp. 10-12.
- 579 Saviano, A., Pisanò, F., 2017. Effects of misalignment on the undrained HV capacity of suction
580 anchors in clay. *Ocean Engineering* 133, 89-106.
- 581 Senders, M., Kay, S., 2002. Geotechnical suction pile anchor design in deep water soft clays.
582 In: Proc of the 7th IBC Deepwater Risers, Moorings and Anchorings Conference. IBC, London,
583 UK, p. 50.
- 584 Statoil, 2015. Hywind Scotland Pilot Park.
585 [https://www.statoil.com/content/dam/statoil/documents/impact-assessment/Hywind/Statoil-](https://www.statoil.com/content/dam/statoil/documents/impact-assessment/Hywind/Statoil-EnvironmentalStatementApril2015.pdf)
586 [Environmental](https://www.statoil.com/content/dam/statoil/documents/impact-assessment/Hywind/Statoil-EnvironmentalStatementApril2015.pdf) Statement April 2015.pdf.
- 587 Steensen-Bach, J., 1992. Recent model tests with suction piles in clay and sand. In: Proc of
588 Offshore Technology Conference. OTC, Houston, Texas, OTC-6844-MS.
- 589 Supachawarote, C., Randolph, M., Gourvenec, S., 2004. Inclined pull-out capacity of suction
590 caissons. In: Proc of the 14th International Offshore and Polar Engineering Conference. ISOPE,
591 Toulon, France, pp. 500-506.
- 592 Supachawarote, C., Randolph, M., Gourvenec, S., 2005. The effect of crack formation on the
593 inclined pull-out capacity of suction caissons. In: Proc of International Association for
594 Computer Methods and Advances in Geomechanics (IACMAG), Turin, Italy, pp. 19-24.
- 595 Tjelta, T., 2015. The suction foundation technology. In: Proc of the 3rd International Symposium
596 on Frontiers in Offshore Geotechnics, Oslo, Norway, pp. 85-93.
- 597 Watson, P., Randolph, M., 1997. Vertical capacity of caisson foundations in calcareous
598 sediments. In: Proc of the 7th International Offshore and Polar Engineering Conference. ISOPE,
599 Honolulu, USA, pp. 784-790.
- 600 Watson, P., Randolph, M., Bransby, M., 2000. Combined lateral and vertical loading of caisson
601 foundations. In: Proc of Offshore Technology Conference. Offshore Technology Conference,
602 Houston, Texas, OTC-12195-MS.
- 603 Zdravkovic, L., Potts, D., Jardine, R., 2001. A parametric study of the pull-out capacity of
604 bucket foundations in soft clay. *Géotechnique* 51 (1), 55-67.
- 605

606 **TABLE**

607 Table 1 Comparison of the geotechnical capacity of caisson in intact and trenching seabed for
 608 the example application

Trench width, w/D	Normalised horizontal capacity factor, N_h		[(1)-(2)]/(1) _{intact}
	UTI (1)	ZTI (2)	
Intact	10.89	7.48	0.313
→ 0	9.75	6.37	0.310
0.25	9.15	5.78	0.309
0.50	8.51	5.14	0.310
0.75	7.90	4.49	0.313
1.00	7.14	3.72	0.313

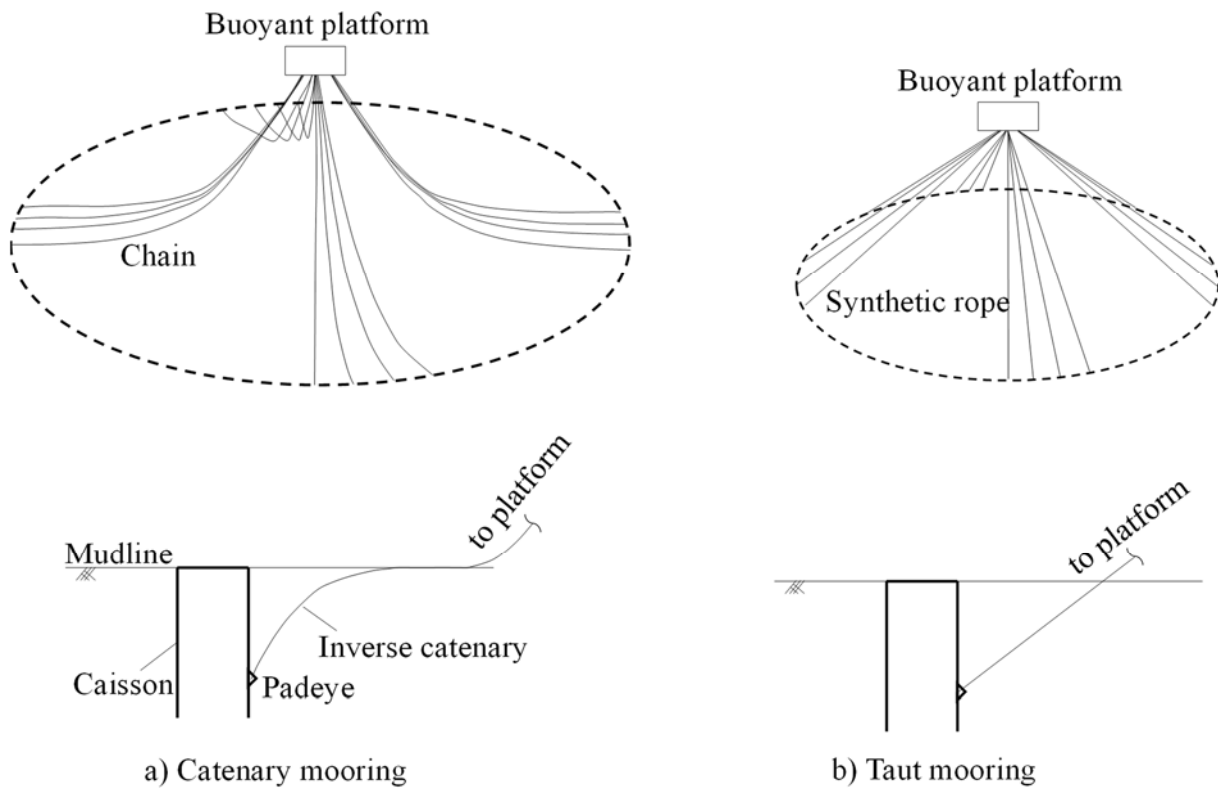
609

610 .

611 **FIGURE CAPTIONS**

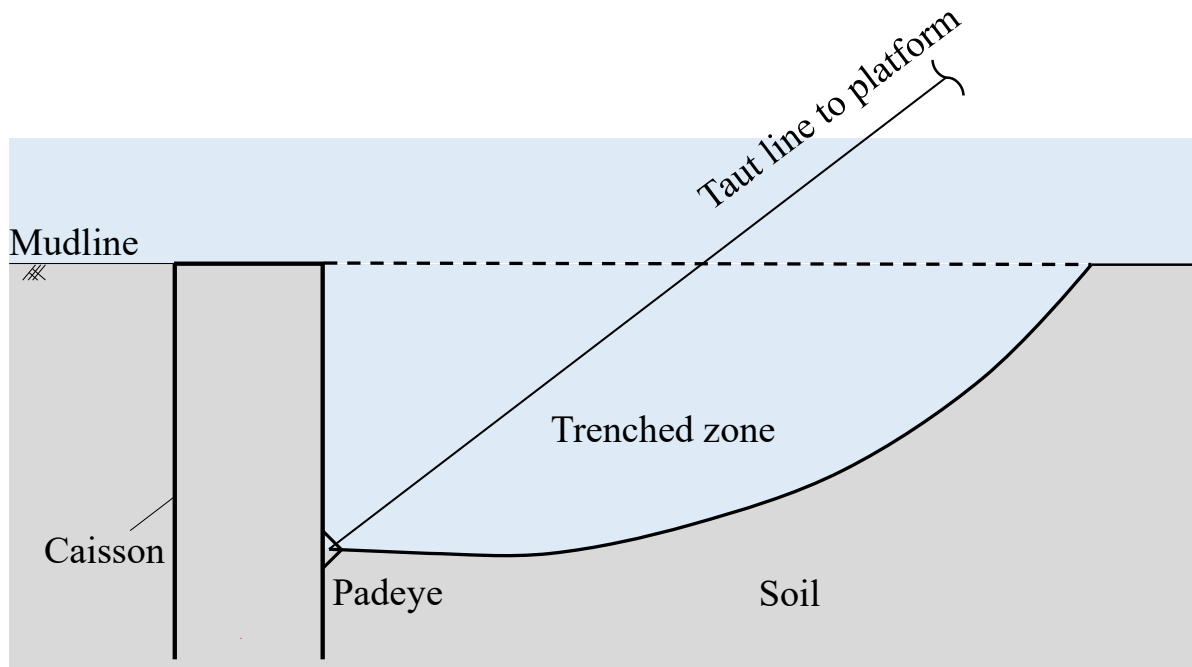
- 612 Figure 1 Mooring line and anchorage arrangements for catenary and taut moorings
- 613 Figure 2 Schematic of seabed trenching around a taut-line mooring (based on case study in
614 Bhattacharya et al. 2014)
- 615 Figure 3 Nomenclature for problem definition
- 616 Figure 4 Example of FE mesh for suction caissons in trenched seabed ($w/D = 0.75$)
- 617 Figure 5 Failure mechanism assumed for a horizontally translating caisson and profile of unit
618 lateral resistance
- 619 Figure 6 Reduction in the pullout and translational capacity of suction caissons with varying
620 trench width
- 621 Figure 7 End bearing capacity factor and horizontal capacity factor for suction caissons in
622 intact and trenched seabed
- 623 Figure 8 Soil flow mechanisms around translating caissons with UTI (Contours of soil
624 movement relative to caisson displacement)
- 625 Figure 9 Soil flow mechanisms around translating caissons with ZTI (Contours of soil
626 movement relative to caisson displacement)
- 627 Figure 10 Components of reduction in load capacity of caissons in trenched seabed with load
628 attachment point at optimal depth for intact seabed
- 629 Figure 11 Depth to optimal load intersection with the centreline for suction caissons in
630 trenched seabed for varying padeye positions
- 631 Figure 12 Example showing dependence of geotechnical capacity on the depth to load
632 intersection point at the centreline and load inclination angle (UTI; $w/D = 0.25$)
- 633 Figure 13 Comparison of V-H failure envelopes for suction caissons in intact and trenched
634 seabed
- 635 Figure 14 Normalised V-H failure envelopes for suction caissons in intact and trenched
636 seabed
- 637 Figure 15 Loading diagram for a translating caisson in trenched seabed
- 638 Figure 16 Effect of padeye offset on the load capacity of the suction caisson if designing for
639 inevitable trenching
- 640 Figure 17 Effect of seabed trenching and gapping conditions on the inclined capacity for the
641 example application based on Bhattacharjee et al. (2014)
- 642

643



644

645 Figure 1 Mooring line and anchorage arrangements for catenary and taut moorings



646

647

648 Figure 2 Schematic of seabed trenching around a taut-line mooring (based on Bhattacharjee et
649 al. 2014 case study)

650

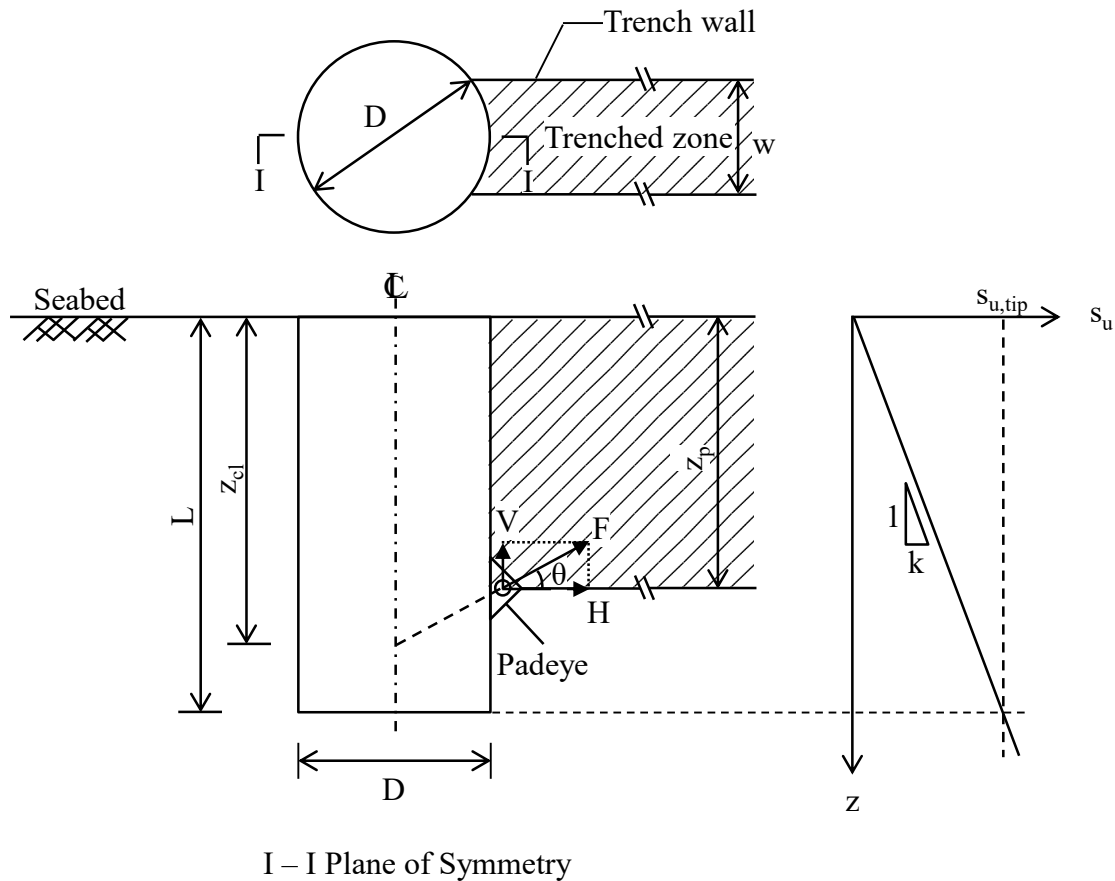


Figure 3 Nomenclature for problem definition

651
652
653
654

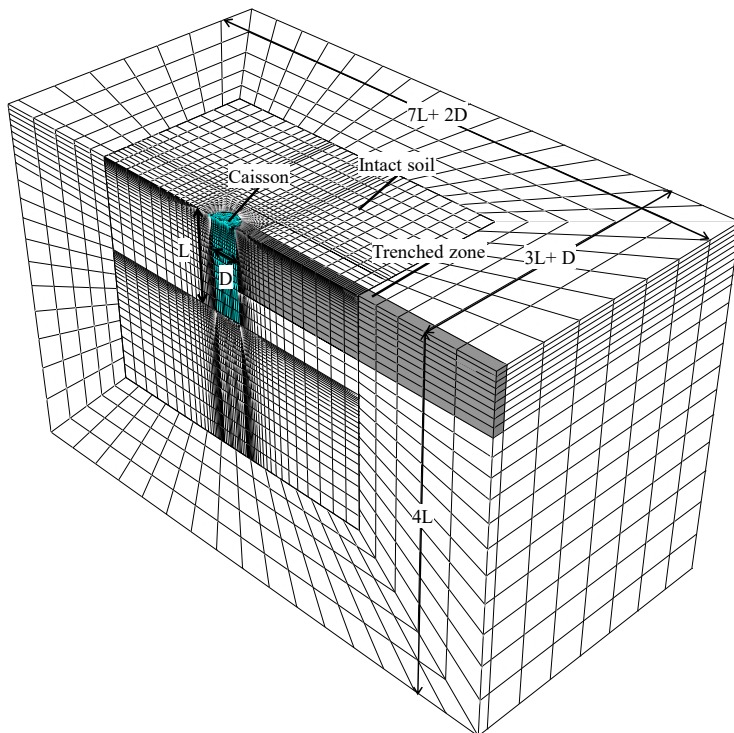
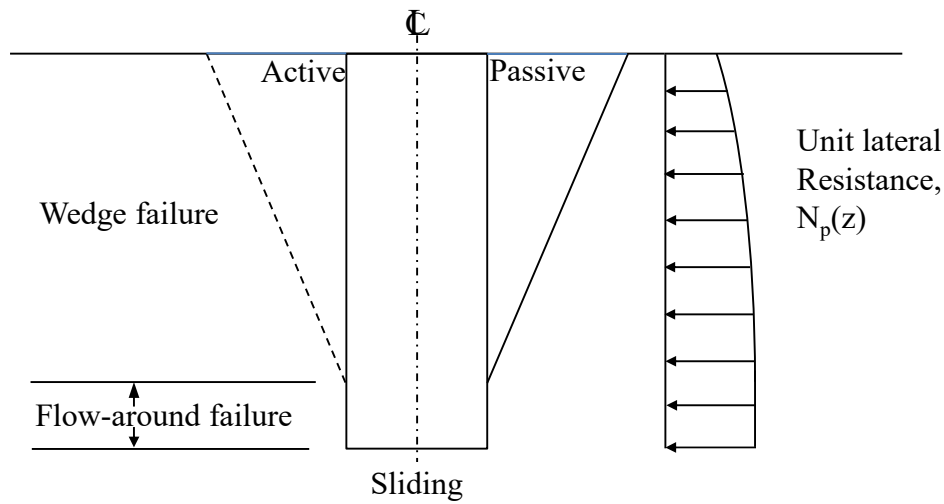


Figure 4 Example of FE mesh for suction caissons in trenched seabed ($w/D = 0.75$)

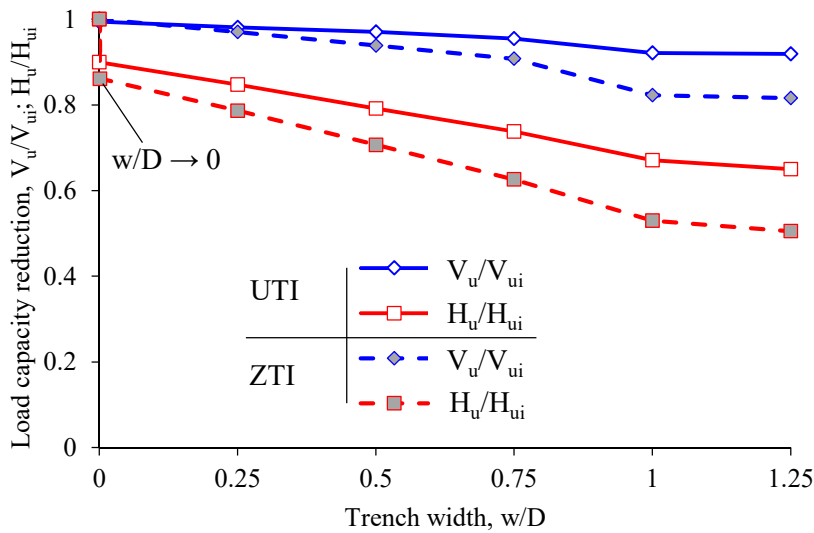
655
656
657
658

659



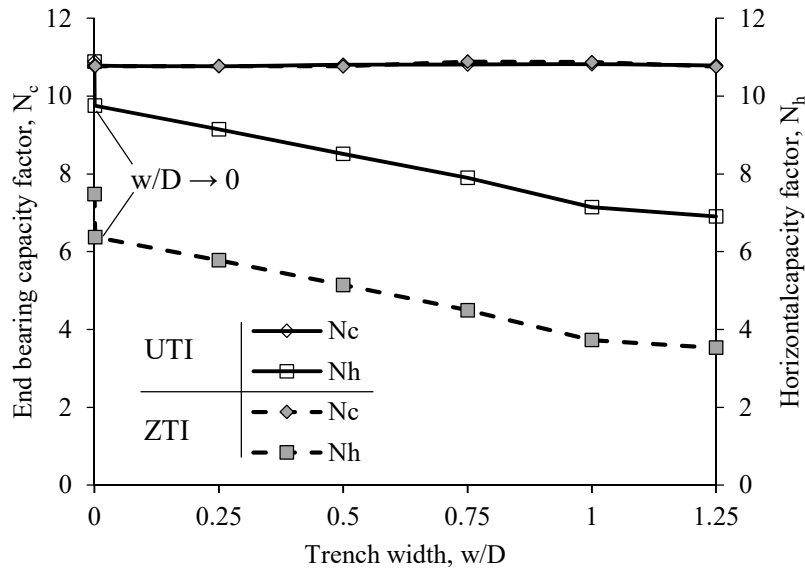
660
661
662
663

Figure 5 Failure mechanism assumed for a horizontally translating caisson and profile of unit lateral resistance



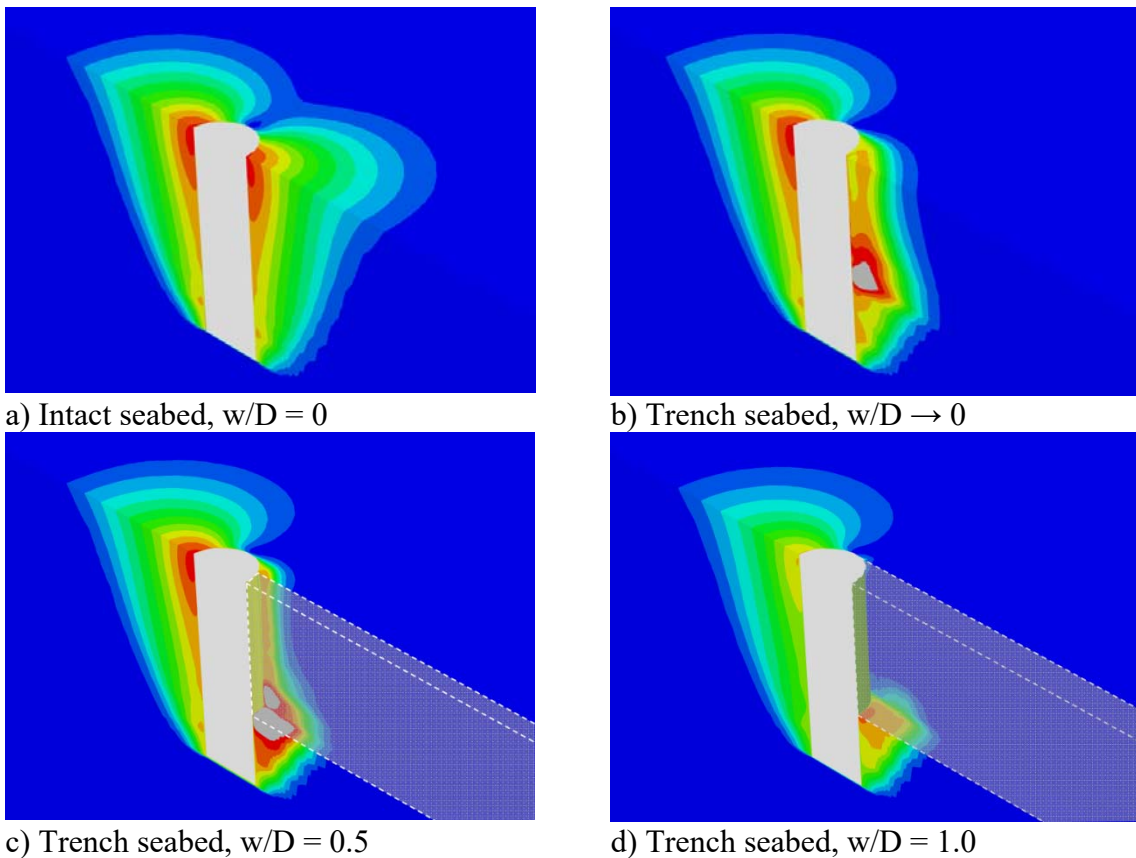
664
665
666
667

Figure 6 Reduction in the pullout and translational capacity of suction caissons with varying trench width



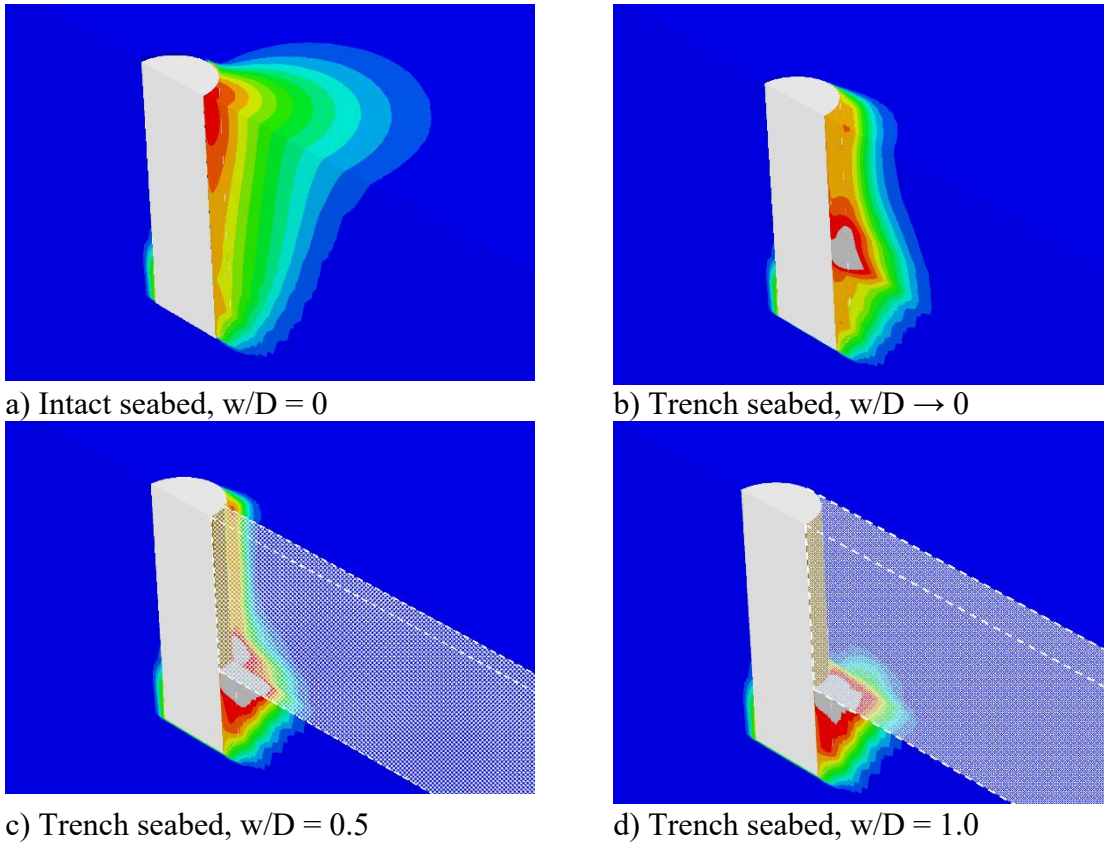
668
669
670
671
672

Figure 7 End bearing capacity factor and horizontal capacity factor for suction caissons in intact and trenched seabed

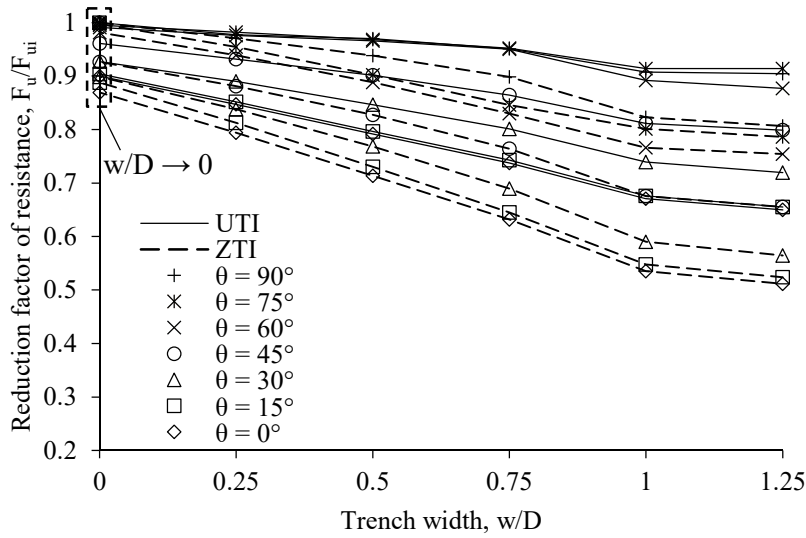


673
674
675
676

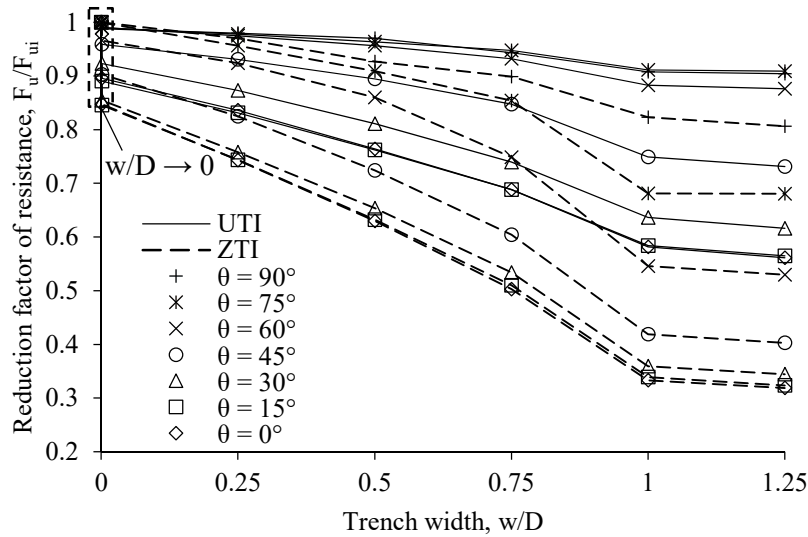
Figure 8 Soil flow mechanisms around translating caissons with UTI (Contours of soil movement relative to caisson displacement)



677
678 Figure 9 Soil flow mechanisms around translating caissons with ZTI (Contours of soil
679 movement relative to caisson displacement)

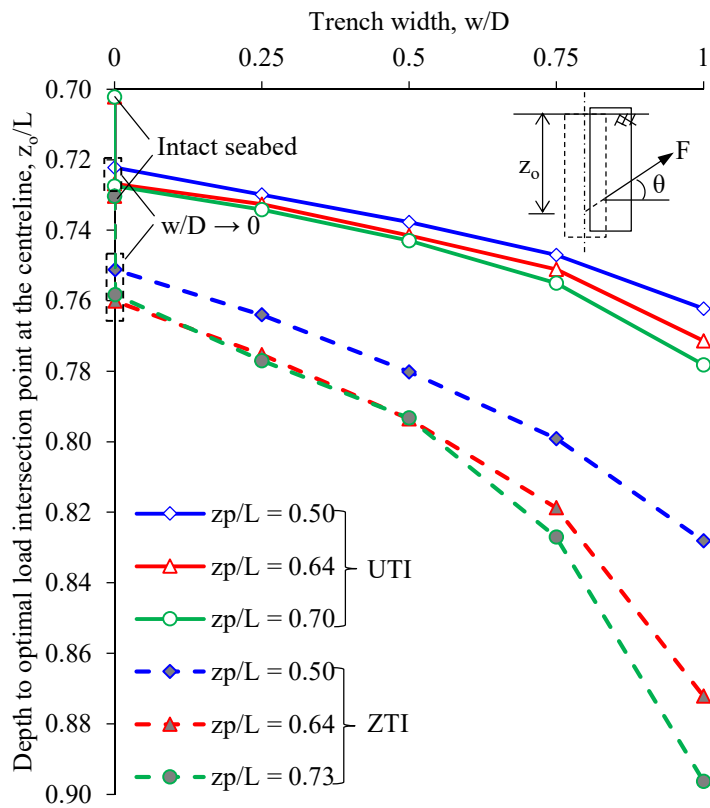


680
681 a) effect of loss of soil support and suction

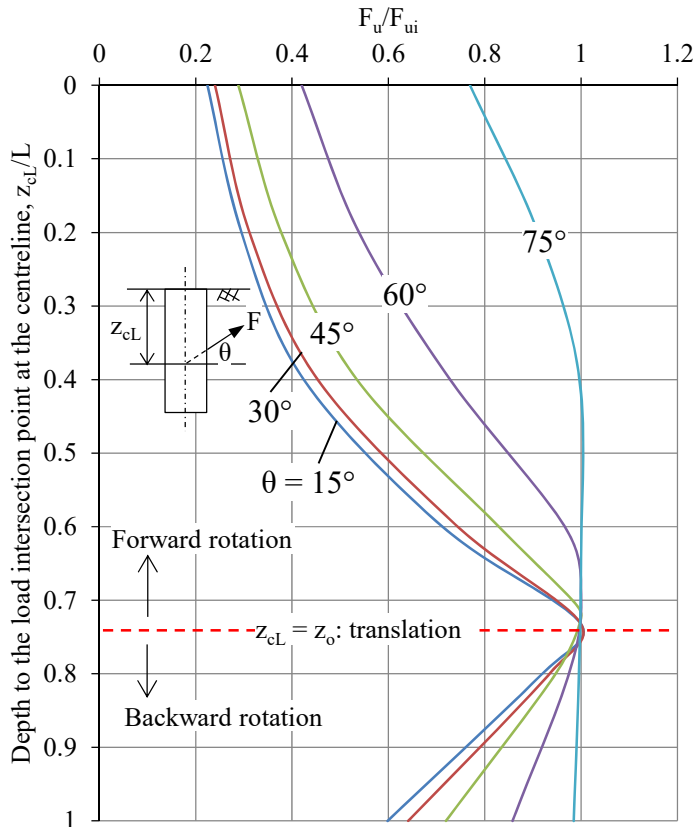


682
683 b) effect of rotation

684
685 Figure 10 Components of reduction in load capacity of caissons in trenched seabed with load
686 attachment point at optimal depth for intact seabed
687

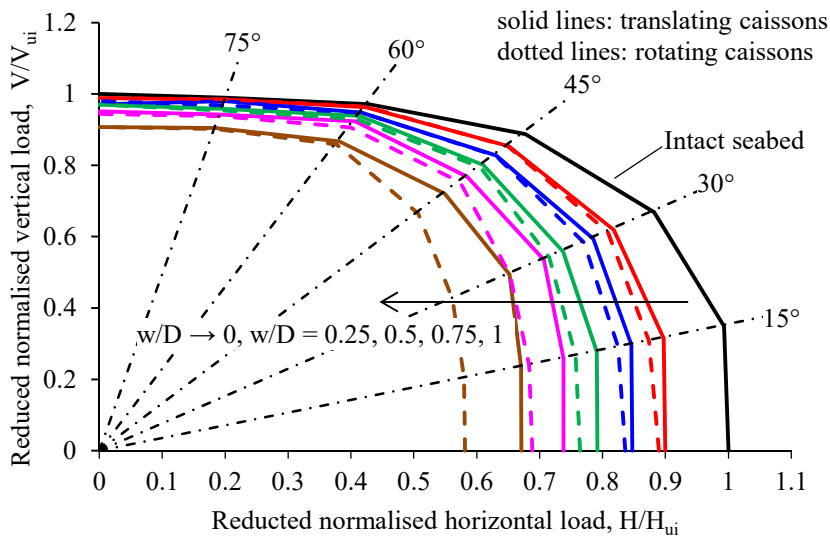


688
689 Figure 11 Depth to optimal load intersection with the centreline for suction caissons in trenched
690 seabed for varying padeye positions
691
692



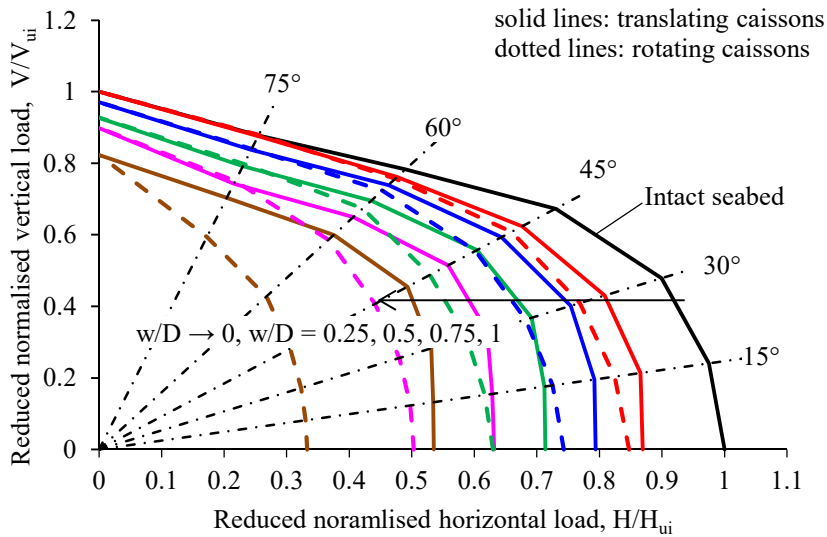
693
694
695
696
697

Figure 12 Example showing dependence of geotechnical capacity on the depth to load intersection point at the centreline and load inclination angle



698
699
700

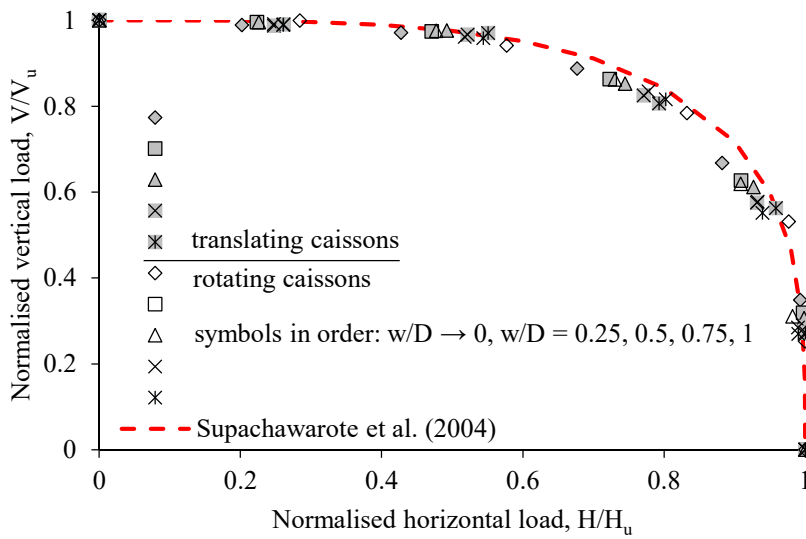
a) unlimited tension interface



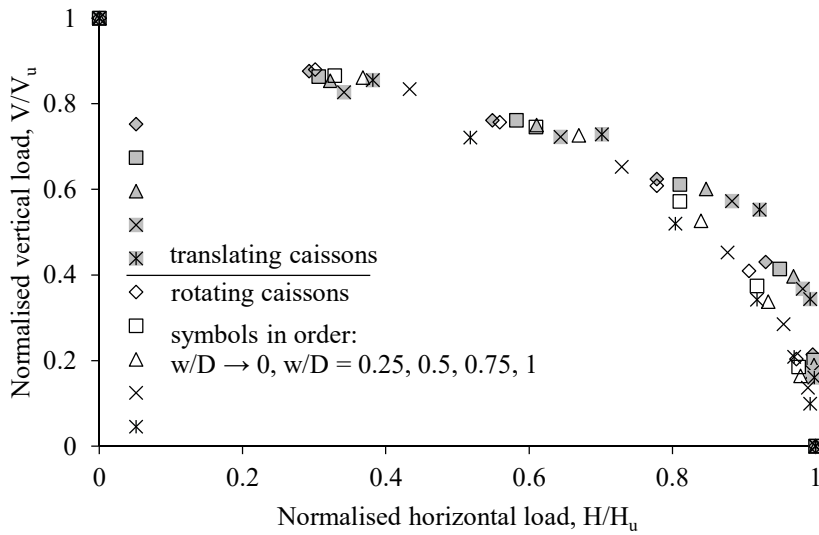
701
702 b) zero-tension interface
703

704 Figure 13 Comparison of V-H failure envelopes for suction caissons in intact and trenched
705 seabed

706
707

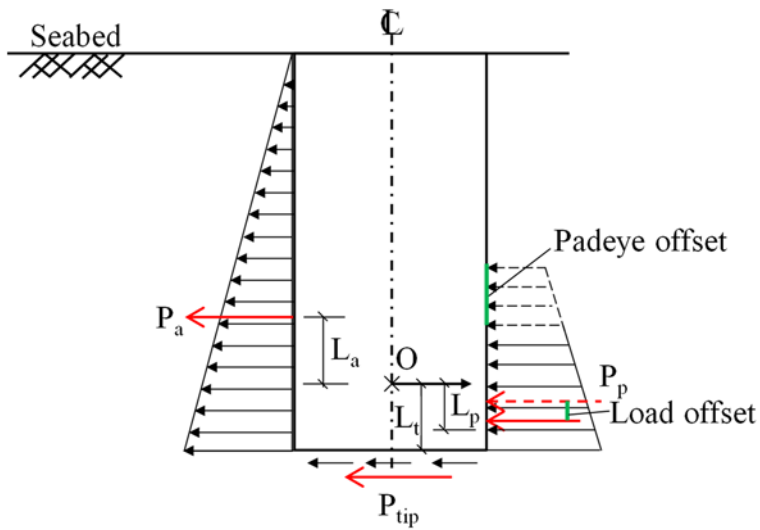


708
709 a) unlimited tension interface

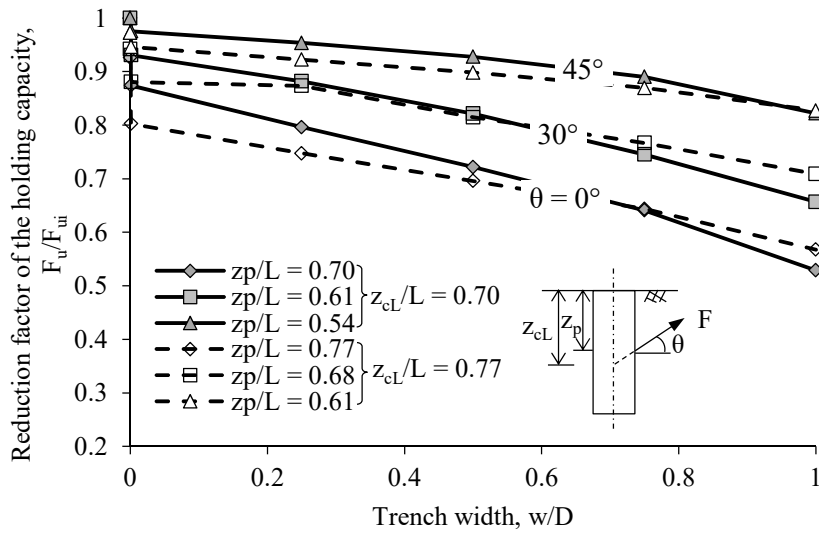


710
711 b) zero-tension interface
712

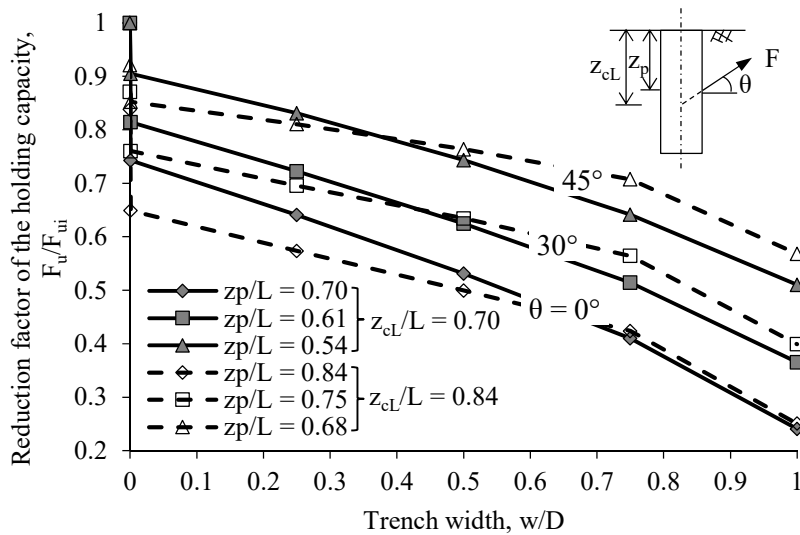
713 Figure 14 Normalised V-H failure envelopes for suction caissons in intact and trenched seabed



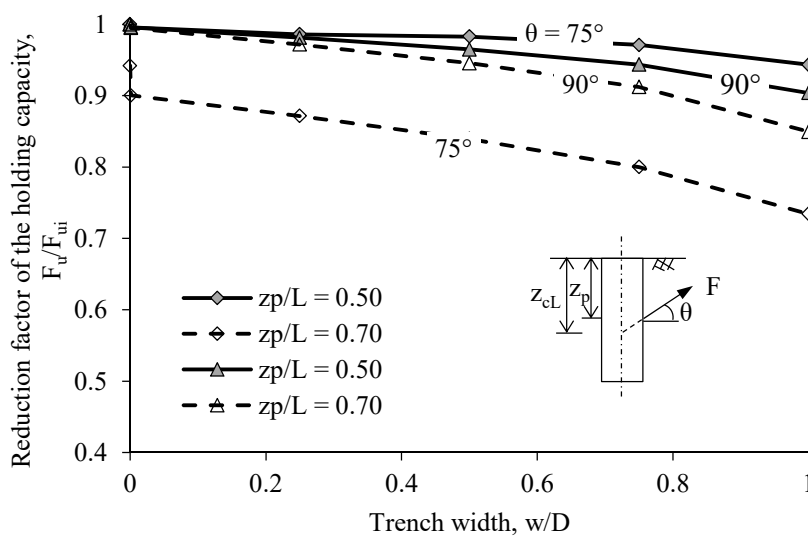
714
715
716 Figure 15 Loading diagram for a translating caisson in trenched seabed
717



718
719 a) $\theta \leq 45^\circ$; unlimited tension interface
720



721
722 b) $\theta \leq 45^\circ$; zero-tension interface
723



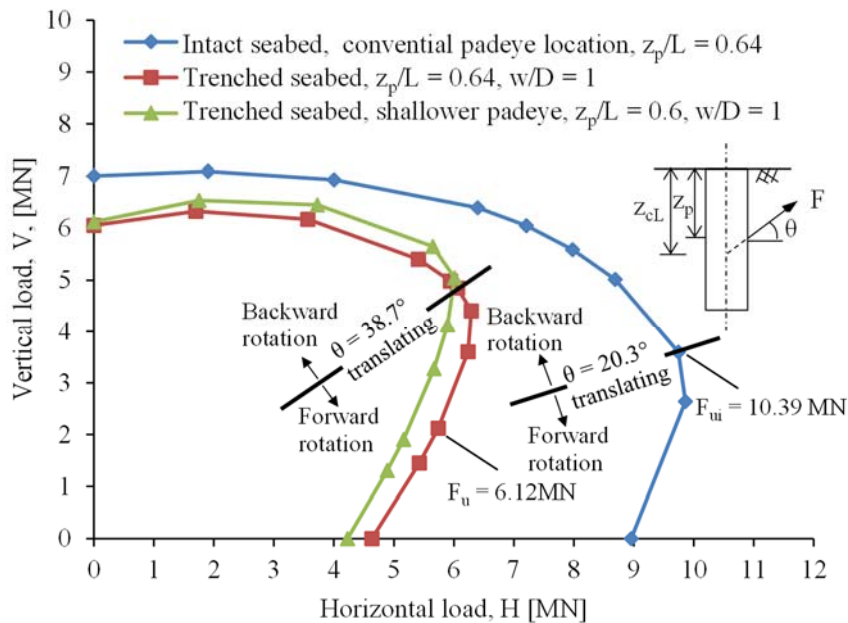
724

725 c) $\theta \geq 75^\circ$; unlimited tension interface

726

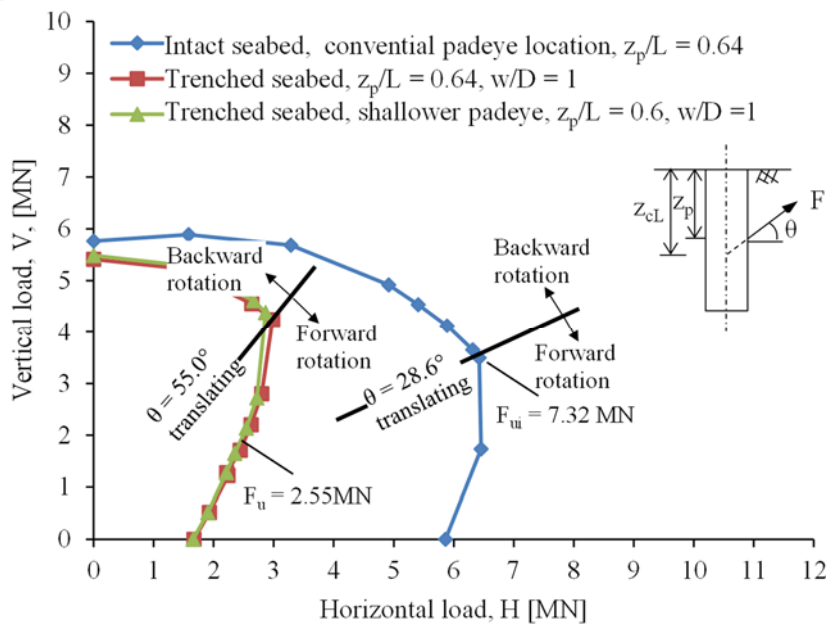
727 Figure 16 Effect of padeye offset on the load capacity of the suction caisson

728



729

730 a) unlimited tension interface



731

732 b) zero-tension interface

733

734 Figure 17 Effect of seabed trenching and gapping conditions on the inclined capacity for the
735 example application based on Bhattacharjee et al. (2014)